euspen's 22nd International Conference & Exhibition, Geneva, CH, May/June 2022
www.euspen.eu

# Measurement-based loop shaping approach of feedback control for high performance direct drives incorporating friction behaviour of guides

Lukas Konietzny[1], Ulrich Schönhoff[1]

[1]*Carl Zeiss SMT GmbH*

*Lukas.Konietzny@Zeiss.com*

**Abstract**

Control systems for roller-bearing-guided direct drives have to deal with varying plant behaviour during one move: Mass behaviour is dominant once the stage is moving with noticeable speed while stiction and stick-slip-effects are dominating the last micron positioning part.

This paper shows a pragmatic measurement-based approach for designing, tuning, and evaluating a control-loop which is both performant and robust facing the different friction behaviours between moving and positioning.

The key is to measure the plant in its two characteristic states - motion and stiction - and to design the controller simultaneously for the two measured plant states. For doing this, two frequency response function (FRF) measurements with different excitation and moving speeds of the axis are acquired using a preliminary controller design. These FRF-measurements show the above-described nonlinear behaviour: Stiction is dominating in low-current and standstill situations while mass dominates once the slide is moving. Alongside appearing parasitic and payload related resonances are considered as well.

To simulate the resulting open-loop-FRFs, the measured plant-FRFs are used as input to a numeric model of the control loop capturing its structure as well as all its tuneable parameters. Therefore, controller design and parametrisation can be modified, and its characteristics can be simulated within seconds without the need of additional measurements.

A cascade of three PI-controllers for current, velocity and position is investigated for faster settling. It turns out that this can be advantageous for settling into a given error window and increased disturbance rejection at low frequencies. Its drawbacks compared to the standard P-PI-approach for position control are an enlarged settling to zero error due to oscillation and increased disturbances around its bandwidth. Therefore, the individual application defines which controller layouts fits best.

Verification measurements in time and frequency domain lastly proofed the performance and showed stable behaviour for all measured friction scenarios.

Control Engineering, Loop Shaping, FRF-Measurement, Sensitivity Function, Stick-Slip-Effect, Roller Bearings, Direct Drives

## 1. Introduction

Precision optics in high performance measurement machines require fast positioning over several decimetres and position accuracy on nanometre level. When using roller bearings for the positioning stages, the settling from micrometres down to nanometre-scale takes place in the sticking regime of the roller bearing. During this transition from moving to sticking the plant behaviour changes significantly between mass- and stiffness-dominance.

This paper shows a measurement-based design approach which takes care of this variant plant behaviour as well as payload related parasitic resonances, to find a controller design that is both performant and stable for the whole movement.
In contrast to standard loop-shaping methods (esp. [1]) the plant is neither considered as ideal nor constant over the movement.

In Chapter 2 the different plant behaviours between moving and creeping are explained.

Chapter 3 then explains the design method itself nearby the controller structure used for the experiments and some general design guidelines for position control.

In Chapter 4 the improvements and drawbacks of a second integrator in the position loop are investigated since this is not a common approach in standard literature [2,3,4,5].

Chapter 5 discusses the overall approach, gives some recommendations of its usage alongside some outlooks and extensions.

## 2. Actuator Force related Friction Behaviour of Roller Guides

Due to their friction behaviour roller guides are highly nonlinear elements in the plant model. Friction during movement differs significantly from sticking during creeping and standstill. The approach of this paper is to approximate this non-linear behaviour with its two extreme representations: Static friction force during movement and spring-like sticking force during standstill. Around these two operating points the model can be assumed as linear and therefore linear methods can be used to design and evaluate a performant and robust controller.

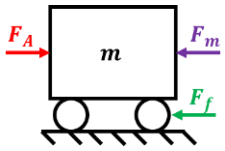


**Figure 1.** Simple model of the drive dynamics

It is prior art to model a roller-bearing-guided direct drive simplified as shown in Figure 1: A moving mass and a normal force ($F_N = m \cdot g$) dependent friction force $F_f$ are representing the drives moving parts while actuator force $F_A$ is working against inertia and friction according (2-1).

(2-1) $$F_A = m \cdot \ddot{x} + F_N \cdot \mu = F_m + F_f$$

Since the friction coefficient μ is low for high quality bearings and normal force is constant in linear actuators $F_f$ might be neglected during motion and the model reduces to a simple moving mass with 180° phase lag and the characteristic "minus-two-Slope":

(2-2) $$\frac{x}{F} = \frac{1}{m \cdot s^2}$$

However, things are different for the last micron "creeping" part of the positioning: Velocity is low and only minimal forces are applied to the moving part. In this part stiction is dominating the plant behaviour:

(2-3) $$\frac{x}{F} = \frac{1}{k}$$

The sticking friction together with the combined stiffnesses of the bearing and the moving parts of the actuator act like a spring connecting the mass to the fixed world.

These two extremes will be investigated more in detail. Figure 2 shows the according model assumptions: For moving state the friction force is neglected, while during creeping only the resulting combined stiffness $k$ is characterizing the systems' dynamics according (2-3).

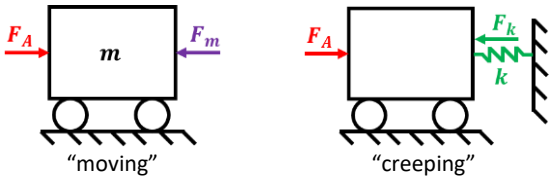


**Figure 2.** Model adaptions for the two extreme plant behaviours

This behaviour can be observed in the plant-FRFs as well. Figure 3 shows the FRFs for the same plant at different excitation levels: For high excitation-forces and motion the described mass-dominated behaviour (2-2) can be identified: "-2-Slope" with -180° phase. Alongside a parasitic resonance around $\omega_p$ shows up.

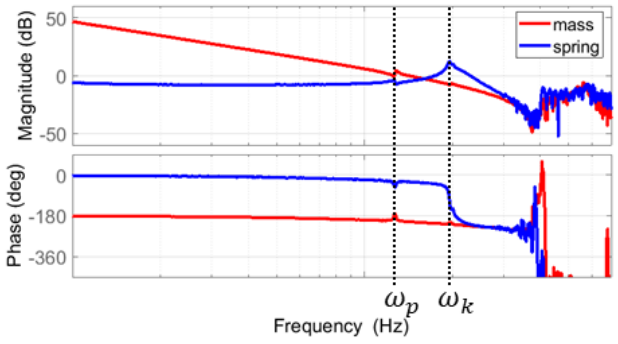


**Figure 3.** Frequency-response-function measurements for mass- and spring-like plant behaviour. At higher frequencies the signal shows high noise which is caused by the low excitation forces. Alongside electronic phase lag occurs.

At low frequencies the magnitude stays at a constant level which can be interpreted as the inverse of a fictive stiffness $k$ according (2-3). It also shows a corresponding resonance at $\omega_k$, like a common mass-spring-system. At this frequency $\omega_k$ the plant behaviour turns back to mass-dominance. Since it is the same plant, also the parasitic resonance at $\omega_p$ can be identified less pronounced although.

## 3. Controller Structure

For position control often cascaded controller structures are used consisting of three sub-control-loops for current-, velocity- and position-control. Since this application focuses on low frequent behaviour and the bandwidth of the current loop is much higher than the bandwidths of the outer loop, current control is neglected in the scope of future chapters.

### *3.1. Open-Loop Transfer-Functions*

Figure 4 shows the given controller structure: Two controllers $C_{pos}$ and $C_{vel}$ are used to control the position and velocity loop while only one position sensor signal is used for both, position- and velocity-loop-feedback.

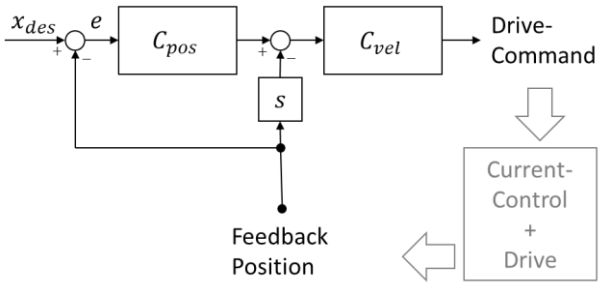


**Figure 4.** Controller structure of the used hardware

It is common to use a P-controller for position- and a PI-controller for velocity-control to not exceed a phase lag of 180° in each loop [1].

(3-1) $$C_{vel} = KP_v + KI_v \cdot \frac{1}{s}$$

(3-2) $$C_{pos} = KP_x$$

With (3-1) and (3-2) the open loop (3-3) becomes:

(3-3) $$C = \underbrace{KP_v * KP_x + KI_v}_{K_P} + \underbrace{KI_v * KP_x}_{K_I} * \frac{1}{s} + \underbrace{KP_v}_{K_D} * s$$

It is obvious that (3-3) is equivalent to a single-loop PID-controller for position control with its parallel gains $K_p$, $K_I$, $K_D$ for proportional, integral, and differential amplification.

Since it is more practical to use the corner frequencies $\omega_{IS}$, $\omega_{DS}$, $\omega_{TS}$ for the integral, differential and lowpass part of the controller instead of parallel gains to design a desired loop-shape the serial equivalent representation for this controller (3-4) will be used in the following chapters.

(3-4) $$C_{PID}(s) = K_{PS} \cdot \frac{1 + \frac{s}{\omega_I}}{\frac{s}{\omega_I}} \cdot \frac{1 + \frac{s}{\omega_D}}{1 + \frac{s}{\omega_T}}$$

### *3.2. Loop-Shaping / Tuning-Process*

For calculating the desired gains of the individual control loops first the equivalent gains of its single-loop-PID representation were calculated using the frequency characteristics method.

It can be shown that the corner frequencies of the serial controller representation can be converted to parallel controller gains and vice versa by comparison of coefficients. The cascade-controller-gains can lastly be calculated out of the parallel controller gains by solving a left unambiguous equation system.

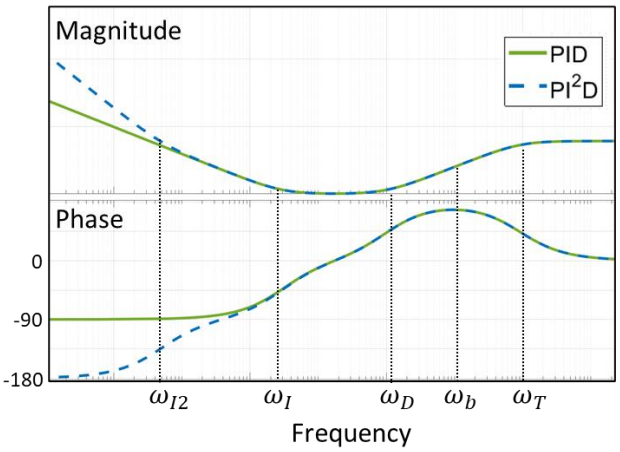


**Figure 5.** Bode representation of a PID and a PI²D controller

Aim of the design is to shape the open loop to maximum gain for frequencies lower than the control bandwidth $\omega_b$ and sufficient phase margin around $\omega_b$. To achieve this for a mass dominated plant like a moving slide of an actuator the controller becomes the typical bathtub-shape shown in Figure 5.

To establish a desired bandwidth a proportional gain factor $K_{PS}$ is used. A differentiator with $\omega_D < \omega_b$. is used to enlarge the phase margin at $\omega_b$. For achieving higher gains an integrator is used with $\omega_I < \omega_b$. Obviously a second integrator with $\omega_{I2} \leq \omega_I$ additionally enlarges the gain at low frequencies and therefore improves the suppression for low frequent disturbances.

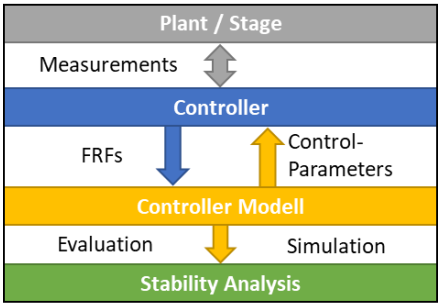


**Figure 6.** Measurement-based design method

In contrast to approximation-based methods (e.g. [1,3]) this approach uses real measurement data instead of simple mass-line- or PT2-simplifications.

The fundamental idea is to use different frequency-response-functions for mass- and friction dominated behaviour (as shown in Ch. 2) at the same time. To do so a simulation-abstraction of the controller has been created. Measured FRFs are used as input to this model and within seconds several loop-shapes for motion and stiction can simultaneously be simulated and evaluated in terms of performance and stability.

Figure 6 shows the described, measurement-based design method. It can be used for different controller-designs and numerous input FRFs of different states.

The final design-parameters can be used subsequently on the real controller hardware. Another measurement iteration finally verifies the desired behaviour.

Figure 7 shows the "design-view" for one PID and one PI²D controller: The controllers have each been applied to two different plants which themselves represent the two extreme plant behaviours described in chapter 2. By doing this the stiffness-related resonance at $\omega_k$ in the "Spring-Like-Plant" can be evaluated and considered as well as other payload related resonances alongside the fundamental mass-line.

The higher gain at low frequencies of the PI²D- compared to the PID-open-loop is visible. In addition, the "bathtub"-shape of the controller is apparent in the spring-like plant-open-loop.

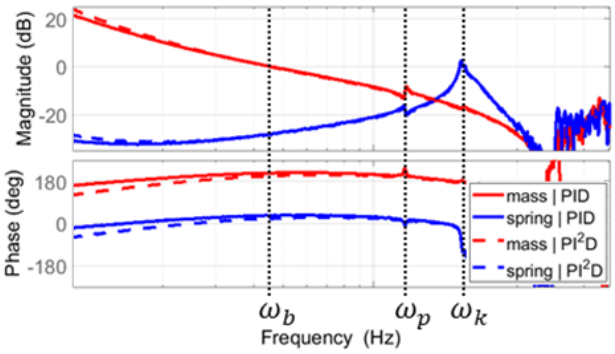


**Figure 7.** Bode-plot of the open loops for both plant behaviour extremes with either PID or PI²D controller

To evaluate the robustness of each approach a sensitivity function plot of the given open loops is used while "robust" behaviour is defined as not exceeding a certain maximum magnitude of the sensitivity function. Such a plot containing the sensitivity functions and the stability margin can be seen in Figure 8 and will be discussed more in detail in the following chapter.

## 4. Extension to PI²D-Control

Figure 10 shows that a significant part of the total positioning time $t_3$ is consumed by the settling to the last micrometre $t_{settle}$. This contrasts with the moving phase, where a large distance is covered with a low and fast settling control error in short time. The slow settling in the sticking state in time domain comes along with significantly decreased open loop gain at low frequencies in frequency domain (Fig. 7), which suggests that increasing the low-frequent open loop gain might improve the settling behaviour in this state. Therefore, the potential of a second integrator in the position-control-loop leading to a PI²D equivalent controller is investigated.

### *4.1. Open-Loop Transfer Functions*

Assuming both Controllers to be PI-Controllers, (3-2) will be extended to (4-1) with a position-control integral gain $KI_x > 0$ :

$$C_{pos} = KP_x + KI_x \cdot \frac{1}{s} \tag{4-1}$$

Having the same structure (Figure 4) with (3-1) and (4-1) the controllers' open loop becomes:

$$C = \underbrace{KP_v * KP_x + KI_v}_{K_P} + \underbrace{(KI_v * KP_x + KP_v * KI_x)}_{K_I} * \frac{1}{s} + \underbrace{KI_v * KI_x}_{K_{I2}} * \frac{1}{s^2} + \underbrace{KP_v}_{K_D} * s \tag{4-2}$$

It equals a serial implemented PI²D controller (4-3) for single loop position control and can be handled as the above-mentioned single loop controller (3-4) extended by a second integrator with a corner frequency at $\omega_{I2S}$:

$$C_{PI2D}(s) = K_{PS} \cdot \frac{1 + \frac{s}{\omega_{IS}}}{\frac{s}{\omega_{IS}}} \cdot \frac{1 + \frac{s}{\omega_{DS}}}{1 + \frac{s}{\omega_{TS}}} \cdot \frac{1 + \frac{s}{\omega_{I2S}}}{\frac{s}{\omega_{I2S}}} \tag{4-3}$$

The main idea of using a second integrator is to improve the suppression of low frequent disturbances. In terms of sensitivity this means a lower magnitude in frequencies below the controller bandwidth, especially below the corner frequency of the second integrator.

Figure 8 shows the sensitivity functions of a standard PID-controller compared to a PI²D-Controller which uses a second integrator with a corner frequency $\omega_{I2S}$. Both are applied to either the mass- or the friction dominated plant-measurement.

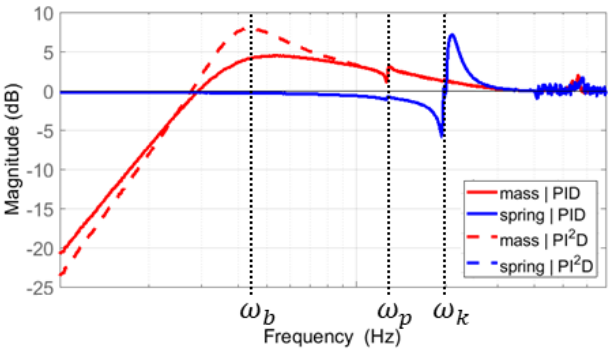


**Figure 8.** Sensitivity-function for both plant behaviour extremes with either PID or PI²D controller

The PI²D controller rejects disturbances up to 5 dB better for low frequencies as its PID implementation. However, the drawback of the second integrator is an increased sensitivity around its bandwidth due to the "waterbed-effect" [1]. This is also visible in Figure 8.

### *4.2. Settling*

Also, in time domain the change in performance appears twofold. This is illustrated by the response of a simple model in sticking state to a disturbance force step in Figure 9. On the one hand the settling becomes faster as anticipated but on the other hand the response now shows a decaying oscillation. The additional integrator has obviously led to an oscillatory pole pair in closed loop. Unfortunately, this oscillation prevents an unconditional faster settling.

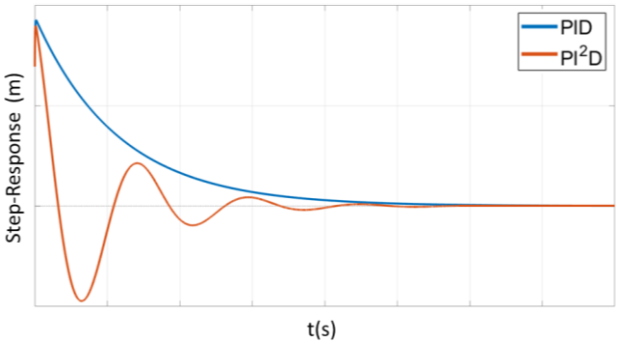


**Figure 9.** Simulation of the step-response of a PID- and PI²D-controlled simple plant model for stiction dominated plant behaviour

However, depending on the required settling threshold, the oscillating response can be of advantage. Figure 10 shows the experimentally determined settling behaviour of the example drive system for the PID and the PI²D controller. For the used settling threshold, the PI²D controller achieves a $\Delta t$ faster settling. Since the settling-time $t_{settle}$ depends only on the constant settling window, while the movement-time $t_{move}$ depends on the individual distance of the movement, $\Delta t$ can become a dominant part of the total movements time consumption. Therefore, a $\Delta t$ faster positioning noticeably optimizes overlying process times.

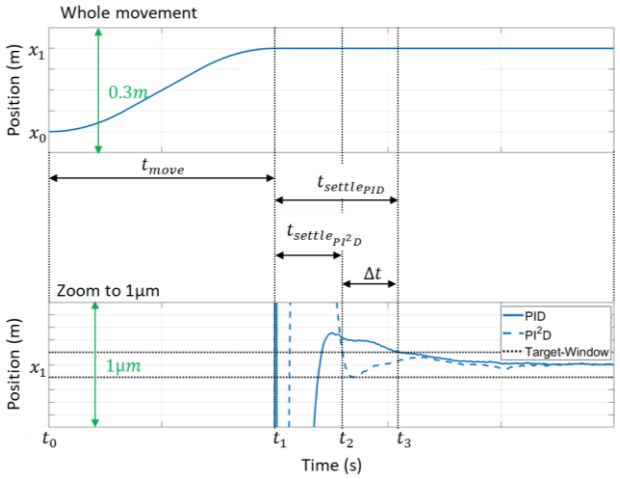


**Figure 10.** Settling after a defined movement for one PID and its extended PI²D design. The lower graph shows the "last-micron-settling".

## 5. Conclusion & Outlook

In this paper a measurement-based approach for designing and tuning position controls for roller-bearing-guided direct drives in high performance applications is shown: By taking two plant behaviours into account which reflect the rolling and sticking states of the roller bearing, performant and robust controls could have been designed. Several measurements demonstrated the functionality of the approach.

Since both PID and PI²D controllers are covered by the shown method the chances and drawbacks of PI²D controllers in the context of roller bearings have been discussed and theory was validated by measurement: It is shown that the settling into a given error window can be speed up by use of a second integrator while settling to zero position error might be enlarged at the same time. Also, disturbance rejection increases on low frequencies but decreases around bandwidth. Therefore, the individual application defines if a P-PI or a PI-PI cascade controller structure should be used.

In future work the transition between mass- and spring-dominated behaviour might be more focused on. It needs to be proved if the two extremes discussed in this paper are sufficient or if some intermediate behaviours should be considered as well. This can be done analogue to the evaluation of the two extremes shown in this paper.

Lastly during the experiments slightly decaying "limit-cycling", showed up when using a PI²D controller for actuators which showed a relatively high stiffness on the last micron. This led to a very high settling time and might be analysed by applying several friction-models to the given simple plant-models.

## References


[1] Schmidt R., Schitter G., Rankers A., van Eijk J. (2020): *The Design of High-Performance Mechatronics*. IOS Press BV, Amsterdam.

[2] Lutz H., Wendt W. (2014): *Taschenbuch der Regelungstechnik*. Verlag Europa-Lehrmittel, Haan-Gruiten.

[3] Zacher S., Reuter M. (2011): *Regelungstechnik für Ingenieure*. Vieweg+Teubner Verlag, Wiesbaden.

[4] Lunze J. (2016): *Regelungstechnik 1*. Springer Verlag, Berlin Heidelberg.

[5] Lunze J. (2016): *Regelungstechnik 2*. Springer Verlag, Berlin Heidelberg.